[Technical Report]

二次精錬炉用 MgO-C れんがの性能に及ぼすフェロクロム添加の影響

Effect of ferrochrome addition on the performance of MgO-C bricks for steel secondary refining furnaces

河野　颯*，**清水公一****，**江上雅之*****
Hayate KAWANO *, Koichi SHIMIZU ** and Masayuki EGAMI ***

要　旨

二次精錬炉用低炭素質 MgO-C れんがへのフェロクロム合金添加がれんがの性能に与える影響を検討した。フェロクロム粉末，Cr_2O_3 粉末，クロム鉱粉末をそれぞれ 3 mass% 添加した試験れんがが作製され，スラグ侵食試験，FeO 侵食試験，スポーリング試験等によりその性能が評価された。その結果，フェロクロム添加により耐スラグ性が 31 % 向上し，黒鉛 3 mass% との併用系では 64 % 改善され，従来の焼成マグクロれんがに近い耐食性が得られることが示された。フェロクロム添加による耐 FeO 性の低下は認められなかったが，耐熱衝撃性は低下することが確認された。微視組織観察および熱力学計算により，フェロクロムから生成したクロム炭化物がスラグと反応し，スラグの高 Cr 化，スピネル固溶体の生成，そして CO ガスの生成により，スラグ接触面に高粘度保護層が形成される機構が考察された。開発された材料は優れた耐 FeO 性と耐食性を有するが，耐熱衝撃性が劣るため，低塩基度スラグかつ高酸素吹込み操業条件での適用が適していることが示唆された。この結果により，製造時 CO_2 排出量の低減と高耐用性を両立する二次精錬炉用耐火物の開発可能性が示された。

Abstract

The effect of ferrochrome addition on the performance of low-carbon MgO–C bricks for secondary refining furnaces was investigated. Test bricks were prepared by adding 3 mass% of ferrochrome powder, Cr_2O_3 powder, and chrome ore powder, and their properties were evaluated through slag corrosion test, FeO corrosion test, and thermal shock test. The results showed that the addition of ferrochrome enhanced slag corrosion resistance by 31%. Furthermore, when combined with 3 mass% graphite, the improvement reached 64 %, nearly matching the corrosion resistance of conventional burnt magnesia–chrome brick. No reduction in FeO resistance was observed with ferrochrome addition. However, a reduction in thermal shock resistance was confirmed. Microstructural analysis and thermodynamic calculations suggested a reaction mechanism in which chromium carbides formed from ferrochrome reacted with the slag, resulting in chromium enrichment in the slag, the formation of spinel solid solutions, and the generation of CO gas. These reactions contribute to the formation of a high-viscosity protective layer at the slag–refractory interface, effectively suppressing slag corrosion. The developed material demonstrated excellent resistance to FeO and slag corrosion. However, due to its lower thermal shock resistance, it is suitable for use in furnace environments with low-basicity slag and high-oxygen blowing (OB) operations, where corrosion is the main cause of refractory wear. These results show the potential for refractories for secondary refining furnaces that offer both reduced CO_2 emissions during production and enhanced durability.

＊　技術研究所 製品プロセス研究センター　Product R&D Center, Technical Research Laboratories
＊＊　技術研究所 製品プロセス研究センター センター長　Center Manager, Product R&D Center, Technical Research Laboratories
＊＊＊　技術研究所 所長　Senior General Manager, Technical Research Laboratories

1　緒言

製鋼プロセスにおける高効率化と鉄鋼製品の高品質化への高まる要求により，二次精錬炉の操業条件は益々過酷化している。特に，Si添加精錬時に生じる，SiO_2含有量の多い低塩基度スラグの生成，そして酸素吹込み時の超高温FeOスプラッシュは炉内耐火物に著しい損耗をもたらす。従来，二次精錬炉の内張りには焼成マグネシア･クロム（マグクロ）質れんがが広く使用されてきたが，スラグ浸潤による構造スポーリングという課題とともに，製造時に1700℃以上の高温で長時間の焼成工程を要し，製造過程での高CO_2排出という環境負荷も問題視されている。

これらの背景から，熱処理温度が低いマグネシア・カーボン（MgO-C）質れんがによる代替[1,2,3]が進められてきた。黒鉛を含有することにより，MgO-Cれんがは溶融スラグに対する濡れ性が低く，構造スポーリングの発生を抑制でき，黒鉛の高熱伝導性により耐熱衝撃性に優れ，マグクロれんがと同等以上の耐用性を発揮するとの報告[4]もある。

しかし，黒鉛含有の有効性の一方で，二次精錬における鋼中への炭素ピックアップ抑制のため，耐火物の黒鉛含有量低減が求められ，低炭素質MgO-Cれんがの適用が増加している。黒鉛の有効性が薄れる中で，MgOは高塩基度スラグには優れた耐食性を示すが，上述した低塩基度スラグには溶解しやすく，耐火物の損耗進行が懸念される。

浅野ら[5]は，マグクロダイレクトボンドれんがへのフェロクロム（Fe-Cr合金）の添加により，耐食性の向上が得られること，そしてその効果が焼成時に生成する$MgCr_2O_4$スピネルがMgO骨材粒子間に充満し緻密な組織をつくることでスラグ浸潤を抑制して得られることを述べている。そこで本研究では，クロム系材料としてフェロクロムをMgO-Cれんがに添加した場合の効果について検討した。

1 Introduction

The growing demands for higher efficiency in steelmaking processes and superior quality of steel products have resulted in increasingly severe operating conditions for secondary refining furnaces. In particular, the formation of low-basicity slag with high SiO_2 content during Si-addition refining, and high temperature FeO splash during the oxygen blowing from the top lance, causes significant erosion of the refractories.

Conventionally, burnt magnesia-chrome bricks have been widely used as the refractories for the inner side walls of secondary refining furnaces. However, they present problems, including structural spalling caused by slag infiltration, and high environmental impact, such as CO_2 emissions due to high temperature (≥1700 ℃) and long-time firing for the production of the brick.

Against this background, replacement with magnesia-carbon (MgO-C) bricks processed at lower temperatures has been advancing[1,2,3]. Due to the presence of graphite, MgO-C bricks exhibit low wettability to molten slag, suppressing the occurrence of structural spalling. The high thermal conductivity of graphite provides excellent thermal shock resistance[4], with some reports indicating service life equivalent to or exceeding that of magnesia-chrome bricks.

Although graphite offers several advantages, the need to suppress carbon pickup in steel during secondary refining has driven the demand for refractories with reduced graphite content, leading to the increased use of low-carbon MgO–C bricks. With the decreasing contribution of graphite to corrosion resistance, concerns arise over accelerated refractory wearing due to the dissolution of MgO in low-basicity slag, despite its excellent resistance to high-basicity slag.

Asano et al.[5] reported that the addition of ferrochrome (Fe–Cr alloy) to magnesia–chrome direct-bonded bricks improves their corrosion resistance, and that this effect is achieved through the suppression of slag infiltration by $MgCr_2O_4$ spinel formed during the firing process, which fills the gaps between MgO aggregate particles and contributes to the formation of a dense microstructure. This work investigates the effects of employing ferrochrome as a chromium-based raw material in MgO-C bricks.

2　実験方法

2.1　試験れんがの調製

各試験れんがは，配合をミキサーで混練し，成形後，250 ℃× 5 h乾燥して作製するもので，電融MgOを90 mass%以上含むMgO-Cれんがをベース材（A）として，それにフェロクロム粉末（Cr含有量60 mass%以上），Cr_2O_3粉末（純度99.0mass%），そしてクロム鉱粉末（Cr_2O_3含有量50 mass%以上）を各3 mass%添加した(B, C, D)（**表1**）。次に，クロム系原料をフェロクロムのみとし，黒鉛を0, 1, そして3 mass%と添加した配合（B-0, B-1，そしてB-3）を作製した。これに，二次精錬炉にて実用されている焼成セミリボンド質マグクロれんが（SRB）を比較材として加えた合計5種類である（**表2**）。

表1及び**表2**に示す合計9種類の試験れんがを上記のように調製したが，両表に含まれるA，さらに**表1**のBと**表2**のB-0は全く同一の組成であるので，評価れんがは合計7種類ということになる。

2　Experimental procedures

2·1　Sample preparation

Test bricks were fabricated by mixing the raw materials, followed by molding and drying at 250 ℃ for 5 h. MgO–C bricks containing over 90 mass% electro-fused MgO were employed as the base brick (A). To this base brick, 3 mass% of each additive − ferrochrome powder (Cr content ≥ 60 mass%), Cr_2O_3 powder (purity 99.0 mass%), and chrome ore powder (Cr_2O_3 content ≥ 50 mass%)− was individually added to produce specimens B, C, and D, respectively (**Table 1**). Next, using only ferrochrome as the chromium-based raw material, mixtures with graphite additions of 0, 1, and 3 mass% (B-0, B-1, and B-3) were prepared. In addition to these, burnt semi-rebonded magnesia-chrome brick (SRB) used in secondary refining furnaces was added as a reference brick, totaling five types (**Table 2**).

A total of nine types of test bricks, as shown in **Tables 1** and **2**, were prepared as described above. However, since the composition of A in both tables, and B in **Table 1** and B-0 in **Table 2**, are completely equivalent, the total number of test bricks for evaluation comes to seven types.

Table 1　Composition of additives for base MgO-C brick A and test bricks B to D used in the 1st test

Test brick			A	B	C	D
Composition /mass%	Base		MgO-C*			
	Additives	Ferrochrome(Cr >60mass%)	−	3	−	−
		Cr_2O_3(>99.0mass%)	−	−	3	−
		Chrome ore (Cr_2O_3 >50mass%)	−	−	−	3

*Fused MgO > 90 mass%

Table 2　Composition of additives for the test bricks B-0, B-1, and B-3 used in the 2nd test, showing also A and SRB as another brick

Test brick			A	B/B-0	B-1	B-3	SRB**
Composition /mass%	Base		MgO-C*				
	Additives	Ferrochrome ***	−	3			
		C (Graphite)	−	−	1	3	

*Fused MgO > 90 mass%, **MgO-Cr_2O_3(MgO/Cr_2O_3=63/24), ***same as that shown in Table1

2.2　特性評価

最初にクロム系原料の種類の違いがかさ密度及び弾性率に及ぼす影響を調べた後，スラグ侵食試験を行った。次にクロム系原料をフェロクロムに絞り，それに黒鉛添加の有無及び量の違いが同じくかさ密度，弾性率に及ぼす影響を調べ，さらにスラグ侵食試験，FeO 侵食試験および熱衝撃試験を実施した。そこでは従来材である焼成マグクロれんがとのスラグ耐食性及び耐 FeO 性の比較を行い，実炉での代替可能性についても検討した。

2.2.1　密度及び弾性率の測定

各試作れんがに対して乾燥後および 1400℃×10 h の熱処理（炭素熱還元）後，20×20×80mm の試験片を用い JIS R2205 に準拠してアルキメデス法により見掛気孔率，かさ密度を測定した。弾性率は超音波パルス法により，音波の伝播速度から算出した。

2.2.2　スラグ侵食試験

台形断面形状の試験片を内張したドラム炉の中央部を，酸素 - プロパンガスバーナーで加熱し回転させながら 1700 ～ 1750 ℃に保持し，1 kg のスラグを投入して 30 min 回転させ，スラグを排出し新たなスラグを再投入する操作を合計 10 回，5 h 繰り返した。なお，用いたスラグの成分は SiO_2 : 30 mass%，CaO : 30 mass%，Al_2O_3 : 20 mass%，FeO : 20 mass% で，塩基度（CaO/SiO_2 比）は 1 である。試験後，試験片断面において溶損された深さを 6 点測定し，平均して溶損深さを算出した後，ベース材料である A の値を 100 とした場合の各試験れんがの溶損深さ比で表した溶損指数により材料間の相対評価を示した。この値が小さいほど耐食性に優れることを示している。

2.2.3　FeO 侵食試験

スラグ侵食試験と同様な装置で同一断面形状の試験片を内張したドラム炉の中央部に鋼製ランスから酸素を吹込みながらドラム炉を回転させ，RH 炉における酸素吹込み操業を模擬した。約 2 min 30 s の酸素吹込みと FeO スラグ排出を合計 10 回繰り返し，約 25 min 間試験した。試験後はスラ

2･2 Testing methods

Initially, the effects of chromium-based raw materials on bulk density and elastic modulus were evaluated, followed by slag corrosion test. Based on these results, ferrochrome was selected for further study as the chromium-based additive. Subsequently, the influence of graphite addition, both its presence and quantity, on bulk density and elastic modulus was examined. In addition, slag corrosion test, FeO corrosion test, and thermal shock test were performed. These properties were compared with those of conventional burnt magnesia–chrome brick to assess the potential of the test bricks as practical alternatives for actual furnace applications.

2･2･1 Physical properties

Apparent porosity and bulk density of each fabricated brick were measured after drying and heat treatment at 1400 ℃ under carbothermal reduction, using the Archimedes method according to JIS R2205 on test pieces of 20×20×80 mm. The elastic modulus was calculated from the propagation velocity of ultrasonic waves.

2･2･2 Slag corrosion test

Using a rotary furnace lined on the inner wall with test pieces, each has a trapezoidal cross-section. The central part of the drum furnace was heated using an oxygen-propane gas burner and maintained at 1700-1750 ℃ while rotating the drum furnace. Then, 1 kg of slag was charged and rotated for 30 min, the slag was discharged, and new slag was recharged. A course of the operations was repeated 10 times for a total of 5 h. The composition of the slag used was SiO_2: 30 mass%, CaO: 30 mass%, Al_2O_3: 20 mass%, FeO: 20 mass%, and the basicity (CaO/SiO_2 ratio) was 1. After the test, the corrosion depth was calculated by averaging six points where was removed by worn-out on the cross-section of the test piece. The corrosion index was calculated to comparatively evaluate the corrosion resistance of the test bricks, expressing the measured corrosion depth of each brick as a ratio, with the corrosion depth of the reference brick (A) being 100. The lower the corrosion index, the higher the corrosion resistance.

2･2･3 FeO corrosion test

By using the same apparatus with the same cross-section arranged in the center of the drum furnace as the slag corrosion test, oxygen blowing operation in the RH degasser was simulated, with oxygen blowing from a steel lance into the center of a rotary furnace. The oxygen blowing for about 2 min 30 s and FeO slag exchange were repeated 10 times,

グ侵食試験と同様な評価方法により侵食深さを測定し，前項同様の方法で溶損指数を算出して評価サンプル間の比較を行った。

2.2.4　熱衝撃試験

高周波誘導炉を用い，40 × 40 × 200 mmの形状の試験片を1600 ℃に保持した溶銑内に90 s浸漬後，20℃の水中に30 s間保持する操作を1サイクルとして合計3サイクル繰り返し，亀裂の発生状況および破断までの繰り返し回数を目視観察により評価した。

3　実験結果

3.1　クロム系原料種類の影響

250 ℃加熱に比べ1400 ℃加熱の場合，見掛気孔率は倍以上の高い数値を示したが，かさ密度の値はそれほど低下せず，特にCr系原料を添加（B, C, D）した場合，その傾向が強かった。また，弾性率もCr系原料を添加したB，Dにおいて1400 ℃加熱により上昇した。使用したCr系原料のうち，Cr_2O_3を添加したCにおいて見掛気孔率の増加量が最も大きく，ベース材と比較して20%以上の増加を示した（**表3**参照）。

図1はスラグ侵食試験後の切断面写真と前記の方法で算出した溶損深さ及び溶損指数を示している。フェロクロム添加れんがBが最も優れ，ベース材Aと比較して31 %の耐食性改善効果が示された。

resulting in a total test time of about 25 min. After the test, the evaluation method was the same as that of the slag corrosion test. The corrosion depth was measured, and a corrosion index was calculated for comparison between the test bricks.

2･2･4　Thermal shock test

Test pieces (40 × 40 × 200 mm) were immersed in molten iron maintained at 1600 ℃ for 90 s, then removed and water-cooled at 20 ℃ for 30 s. This sequence of operation was repeated three times. Crack formation and the number of cycles until spalling were visually evaluated.

3　Results

3･1　Effect of Cr-based materials

As shown in **Table 3**, the test bricks with heat treatment at 1400 ℃ resulted in more than twice the apparent porosity compared to those dried at 250 ℃. However, the bulk density did not decrease significantly, and this tendency was particularly increased in samples with Cr-based materials (B, C, and D). The elastic modulus increased after 1400 ℃ treatment for samples B and D with Cr-based materials. Among the Cr-based raw materials used, sample C with Cr_2O_3 exhibited the most pronounced increase in apparent porosity, showing an enhancement of over 20 % relative to the base brick.

Figure 1 shows the appearance of the specimen cut surface obtained after the slag corrosion test, with the corrosion depth and index calculated using the previously described method. Brick B, containing ferrochrome, had the highest corrosion resistance, exhibiting 31% improvement compared to the base brick A.

Table 3　Porosity and modulus of elasticity (MOE) for test bricks (including A) heat-treated at 250 ℃×5 h (I)and 1400 ℃×10 h (II) in both 1st and 2nd tests

Test brick	A		B/B-0		C		D		B-1		B-3		SRB
Condition	I	II	I	II	I	II	I	II	I	II	I	II	-
Bulk density　/g-cm^{-3}	3.23	3.21	3.26	3.27	3.25	3.20	3.28	3.23	3.25	3.24	3.22	3.24	3.22
Apparent porosity /%	3.5	7.7	4.1	8.5	4.2	10.1	2.9	8.9	3.9	7.9	3.2	7.0	14.2
MOE　/MPa	85.6	71.8	85.2	88.5	80.8	76.4	95.1	76.8	75.7	75.5	76.5	68.4	48.3

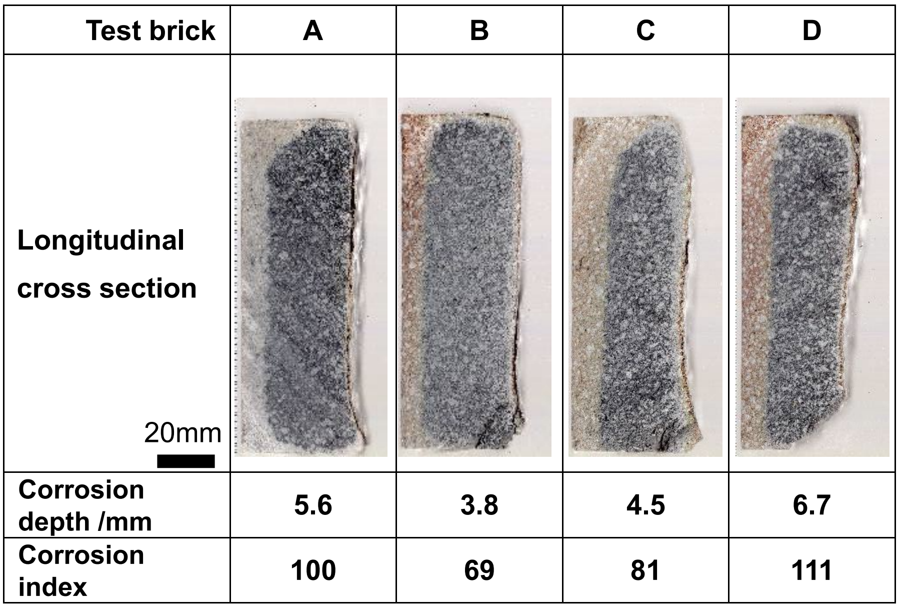

Test brick	A	B	C	D
Longitudinal cross section				
Corrosion depth /mm	5.6	3.8	4.5	6.7
Corrosion index	100	69	81	111

Fig. 1 Results of rotating drum slag corrosion test, showing appearance of the specimen cut surface to measure the corrosion depth for the test bricks of A, B, C, and D.

3.2 黒鉛量の影響

250 ℃加熱と比べ1400 ℃熱処理後の場合，見掛気孔率はほぼ倍程度高くなり（**表 3**），かさ密度も全体的に増大した。フェロクロム添加系において，黒鉛量の増加により，1400 ℃加熱後の弾性率は段階的に低減した。これは黒鉛の低弾性率に起因すると考えられる。また，1400 ℃加熱後の見掛気孔率は黒鉛を3 %添加したB-3において最も低く（7.0%），緻密化の促進を示した。

図 2 にスラグ侵食試験後の切断面写真と前記の方法で算出した溶損深さ及び溶損指数を示す。フェロクロム添加配合は黒鉛量の増加と共に耐食性が顕著に向上し，特に黒鉛3 %添加したB-3において，ベース材Aと比較して64 %の耐食性改善が確認された。この結果は，低炭素質MgO-Cれんがにフェロクロムの添加と適量の黒鉛添加を併用することで，低塩基度スラグに対して焼成マグクロれんがSRBに近い耐食性を発現させることが可能であることを示している。

3･2 Effect of graphite content

The test bricks subjected to heat treatment at 1400 ℃ resulted in nearly double the apparent porosity and increased bulk density compared to those dried at 250 ℃ (**Table 3**). The elastic modulus decreased progressively with increasing graphite content in the ferrochrome-added system. This phenomenon is attributed to the low elastic modulus of graphite. Brick B-3 with 3% graphite showed the lowest apparent porosity (7.0%) after 1400 ℃ treatment, indicating enhanced densification.

Figure 2 shows the appearance of the specimen cut surface obtained after the slag corrosion test, with the corrosion depth and index calculated using the previously described method. Test bricks with ferrochrome addition exhibited marked improvement in corrosion resistance with increasing graphite content. Test brick B-3, containing 3 % graphite, had 64 % higher corrosion resistance compared to base brick A. These results indicate that the combined use of ferrochrome and an appropriate amount of graphite in low-carbon MgO-C bricks can achieve corrosion resistance against low-basicity slag approaching that of burnt magnesia-chrome bricks (SRB).

Test brick	A	B/B-0	B-1	B-3	SRB
Longitudinal cross section 20mm					
Corrosion depth /mm	5.6	3.8	2.9	2.0	1.1
Corrosion index	100	69	52	36	19

Fig. 2 Results of rotating drum slag corrosion test, showing appearance of the specimen cut surface to measure the corrosion depth for the test bricks of A, B-0, B-1, B-3, and SRB.

3.3　微視構造観察とX線回折による生成相の同定

図2に示したスラグ侵食試験後のSEM-BEI（back-scattered electron image）とEPMAによる元素マップを**図3**に示す。フェロクロムを添加したB-0，B-1及びB-3においては，スラグ接触面表層にCr濃度の高い化合物の存在が確認された。これは添加したフェロクロムとスラグの反応により生成したものと考えられた。また，輝度の高い，未反応フェロクロムの点在も確認された。**表4**は**図3**にそれぞれ1a～3a，1b～3bで示す6つのスポットそれぞれの化学成分を示している。**表4(a)**に示す結果から，1a～3aの化合物は炭素を20～25 mass% 含むFeCr系炭化物であり低酸素雰囲気下で周囲の炭素との反応により生成したものと推定される。さらに，**表4(b)**に示す1b～3bの成分分析の結果よりFeCr化合物から，スラグ中にCrが溶出しその周辺に(Mg,Fe)(Cr,Al)$_2$O$_4$型のスピネル固溶体を形成しているものと推定され，周囲のCr濃度の上昇も元素マップにおいて観察されている。加えて，B-0, B-1，B-3ではスラグ中のフェロクロムとの反応生成物には気泡の生成が認められた。

3•3 Microstructure and phase analysis by XRD

Figure 3 presents SEM-BEI (back-scattered electron image) and EPMA element mapping of the test bricks after the slag corrosion test shown in **Fig. 2**. In test bricks B-0, B-1, and B-3 containing ferrochrome, compounds enriched in Cr were observed at the slag reaction surface. These compounds are presumed to have formed through reactions between the added ferrochrome and the slag. Additionally, bright regions corresponding to residual ferrochrome particles were also identified. Table 4 shows the spot chemical analysis results of six specific spots indicated in **Fig. 3** as 1a–3a and 1b–3b. According to the results in **Table 4(a)**, the compounds at spots 1a–3a are Fe-Cr carbides containing 20–25 mass% carbon, which are considered to have formed via reactions with surrounding carbon under low oxygen conditions. Furthermore, based on the compositional analysis in **Table 4(b)**, it is considered that Cr was dissolved from the Fe–Cr compounds into the slag, leading to the formation of (Mg, Fe)(Cr, Al)$_2$O$_4$ spinel solid solutions surrounding the Fe-Cr compounds. This interpretation is supported by the elevated Cr concentrations observed in the elemental maps. In addition, bubble formation was observed in the reaction products between the slag and ferrochrome in samples B-0, B-1, and B-3.

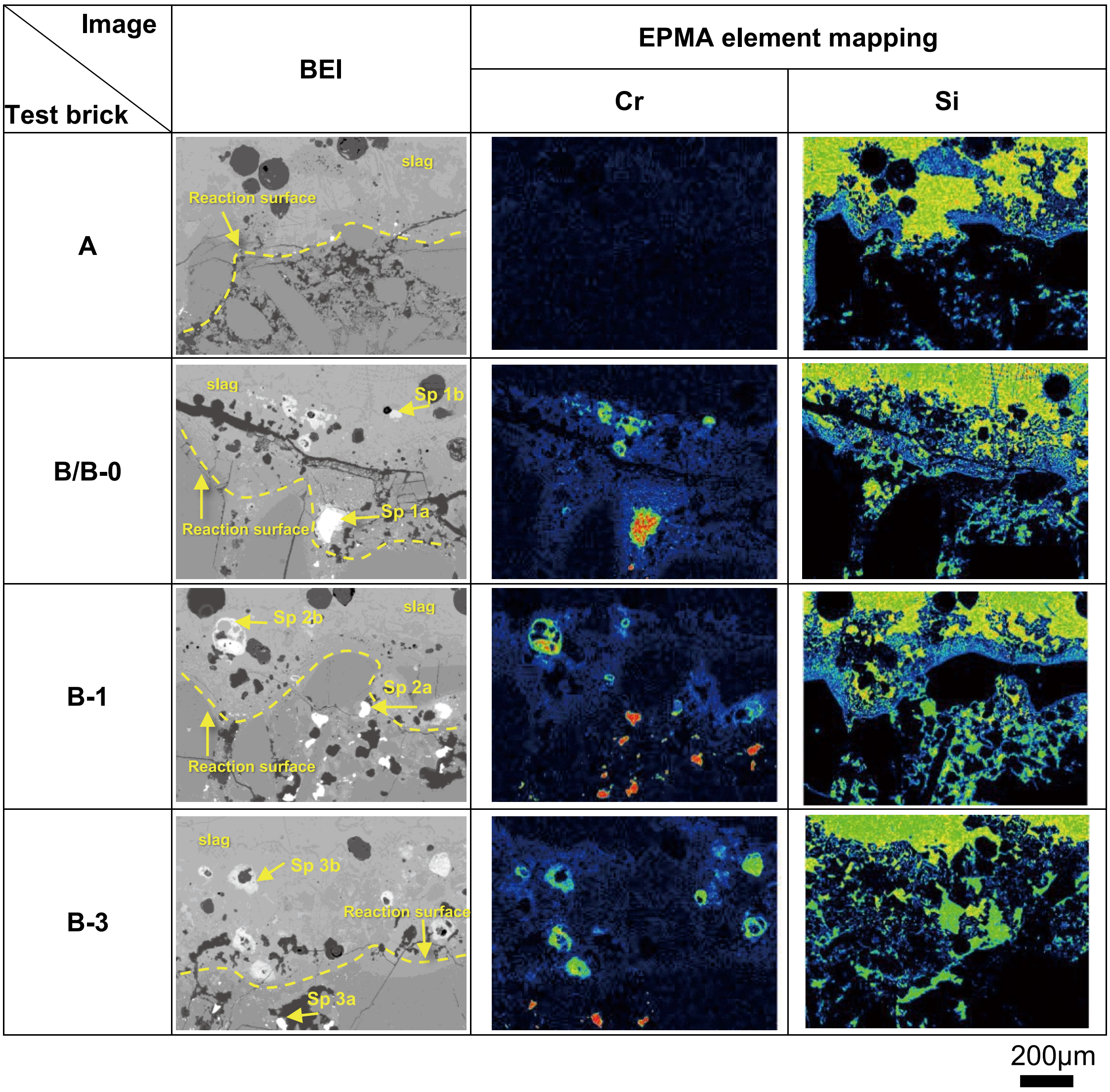

Fig. 3 SEM-BEI (back-scattered electron image) and EPMA element mapping of the test bricks A, B-0, B-1, and B-3 after the rotating drum slag corrosion test, showing slag contact surface in the upper side of each BEI. The arrows in the images also indicate the reaction surface and the positions of spot analysis.

Table 4 Results of spot chemical analysis of the bricks B-0, B-1, and B-3 after slag corrosion test, showing chemical composition of spots 1a to 3a of carbide phase in (a) and phase composition of spots 1b to 3b of oxide phase in (b), both in the BEIs shown in Fig.3

(a) (mol%)

Element Spot/Brick	Fe	Cr	C
1a/B-0	18.9	61.1	20.0
2a/B-1	17.8	57.4	24.9
3a/B-3	15.5	59.7	24.9

(b) (mol%)

Component Spot/Brick	MgO	Al_2O_3	Fe_2O_3	Cr_2O_3
1b/B-0	39.8	9.1	9.6	41.5
2b/B-1	42.4	5.1	7.2	45.3
3b/B-3	40.7	3.4	9.9	46.0

スラグ接触面より20 mm程度内側部分の試験後試料のXRDパターンを**図4**に示す。フェロクロムを添加した全ての試験片において，クロム炭化物であるCr_3C_2および（$(Fe,Cr)_7C_3$の回折ピークが確認された。さらに黒鉛ピークは添加量の増大と共に強さ（ピーク高さ）を増している（B-1及びB-3）が，一方で炭化物のピーク強度は黒鉛添加量に依存せずほぼ一定であったことから，これら炭化物形成に用いられる黒鉛量は元々MgO-Cれんがに含まれる黒鉛量で充分であり追加した黒鉛は遊離黒鉛の増大に寄与するのみであったことが判明した。

Figure 4 shows the XRD patterns of the test bricks at a distance of 20 mm from the contact surface with slag in the rotating drum slag corrosion test. In all specimens with ferrochrome, diffraction peaks corresponding to chromium carbides Cr_3C_2 and $(Fe, Cr)_7C_3$ were detected. The intensity of the graphite peaks increased with the amount of added graphite (B-1 and B-3), whereas the peak intensity of the carbides remained nearly constant regardless of the graphite addition amount. These results suggest that the original graphite content in the MgO-C bricks was sufficient for carbide formation, and that the added graphite primarily contributed to the increase in free graphite.

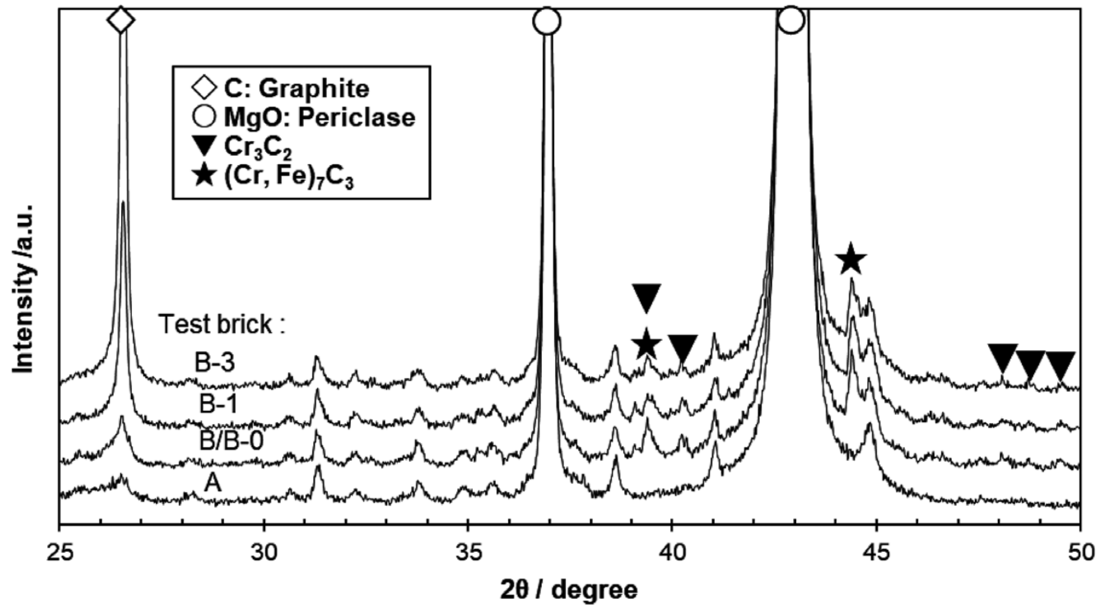

Fig. 4 XRD patterns of the test bricks A, B-0, B-1, and B-3 in a position 20mm apart from the contact surface with slag in the rotating drum slag corrosion test.

3.4　耐FeO性

試験後の切断面外観と侵食深さの測定に基づき前記の方法で算出した溶損深さ及び溶損指数を**図5**に示す。焼成マグクロれんががSRBと比較して全ての試験片において優れた耐FeO性を示した。一般的にMgO-Cれんがにおいて黒鉛やその他の原料を添加すると酸化や低融点化により耐FeO性の低下が懸念されるが，フェロクロム添加による耐

3･4　Corrosion resistance against FeO

Figure 5 shows the appearance of the specimen cut surface obtained after the FeO corrosion test, with the corrosion depth and index calculated using the previously described method. All test bricks had superior FeO resistance compared to the burnt MgO-Cr_2O_3 brick SRB. In general, the addition of graphite or other raw materials to MgO–C bricks raise concerns about reduced FeO resistance due to oxidation or the formation of low-melting phases.

FeO 性の低下は認められず，逆に若干の向上傾向が観察された。添加したフェロクロム及び黒鉛が少量だったため，酸化や低融点化が回避されたものと思われた。

However, no deterioration in FeO resistance was observed with the addition of ferrochrome and graphite. On the contrary, a slight improvement was noted. It is presumed that the oxidation and the formation of low-melting phases were suppressed due to the small amounts of added ferrochrome and graphite.

<table>
<tr><th>Test brick</th><th>A</th><th>B/B-0</th><th>B-1</th><th>B-3</th><th>SRB</th></tr>
<tr><td>Longitudinal cross section
20mm</td><td colspan="5">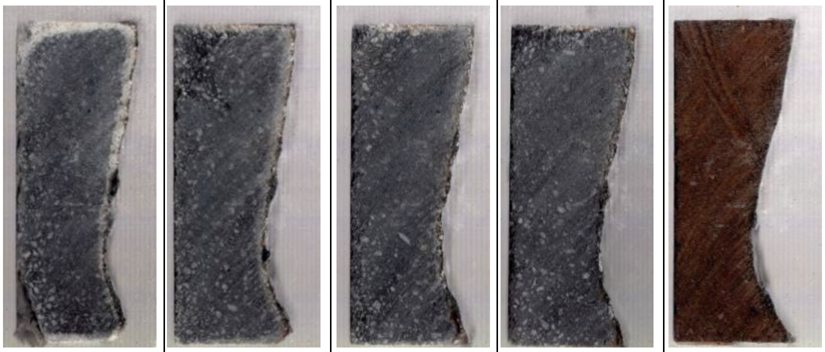</td></tr>
<tr><td>Corrosion depth /mm</td><td>14.6</td><td>14.6</td><td>14.1</td><td>13.6</td><td>18.3</td></tr>
<tr><td>Corrosion index</td><td>100</td><td>100</td><td>96</td><td>93</td><td>138</td></tr>
</table>

Fig. 5 Results of FeO corrosion test, showing appearance of the specimen cut surface to measure the corrosion depth for test bricks of A, B-0, B-1, B-3, and SRB

3.5　耐熱衝撃性

熱衝撃試験の結果として，試験後試片の外観および破断までの繰り返し回数を**図 6** に示す。フェロクロムを添加した B-0, さらに黒鉛を添加し弾性率が低減した B-1, B-3 は 2 サイクル目で試料が破断したが，A は 3 サイクル終了時まで目立った亀裂が入らなかった。この結果はフェロクロムが反応して形成されるクロム炭化物や鉄クロム複合炭化物に起因すると考えられ，れんが全体の見掛上の弾性率が黒鉛添加により低減しても，局所的に存在するこれらの高弾性率の炭化物相が応力集中源として作用することによる脆化の増大により耐熱衝撃性が低下したものと考えられた。

3·5 Thermal shock resistance

As a result of the thermal shock resistance test, the appearance of the test pieces after the test and the number of cycles to spall are shown in **Fig. 6**. Spalling occurred during the second cycle in test brick B-0, which contained ferrochrome, as well as in B-1 and B-3, where graphite had been added to reduce the elastic modulus. In contrast, the test brick A exhibited no significant cracking even after the third cycle. This behavior is attributed to the formation of chromium carbides and iron–chromium composite carbides generated through the reaction of chrome-ferroalloy. Although the overall elastic modulus of the bricks was reduced by the addition of graphite, the locally formed carbide phases with high elastic modulus acted as stress concentrators, thereby promoting embrittlement and decreasing thermal shock resistance.

Test brick	A	B/B-0	B-1	B-3
Appearance after test 40mm				
Number of cycles to spalling	>3	2	2	2

Fig. 6 Results of thermal shock test, showing the appearance of test pieces after test and number of cycles to spall for the test bricks of A, B-0, B-1, B-3, and SRB.

4 考察

4.1 耐食性向上のメカニズム

図 7 に，熱力学計算によって 1400 から 1700 ℃における温度域でのスラグとクロム炭化物が反応した際の安定相割合を求めた結果を示す。反応系は，SiO_2–Al_2O_3–CaO–FeO 組成スラグに MgO が溶解したスラグと，クロム炭化物を単一相 Cr_7C_3 とした単純化モデルで構築した。図から，1700 ℃を超える温度での侵食試験中にスラグに加えて，スピネル固溶体と CO ガスが安定相として存在することが予想できた。Cr_7C_3 と前記したスラグ成分の反応により，主として (Fe,Mg)(Cr,Al)$_2$O$_4$ 組成を有するスピネル固溶体が生成すると考えられる。この反応過程において，炭化物中の炭素の酸化による CO ガスの発生が考えられた。実際に**図 3** で示した侵食試験後のスラグ接触面において観察された FeCr 残渣内部の気泡は，この熱力学計算で予測された CO ガス発生によるものと解釈できた。さらに，Cr 炭化物の一部は CrOx としてスラグ中に溶解し，温度の上昇に伴ってスラグ中の Cr 濃度を増加させることも確認された。

4 Discussion

4･1 Mechanism of improved corrosion resistance

Figure 7 presents the results of thermodynamic calculations that determine the stable phase fractions formed during the reaction of slag and chromium carbide within the temperature range of 1400–1700 ℃. The reaction system was modeled using simplified composition, in which the slag consisted of SiO_2–Al_2O_3–CaO–FeO with dissolved MgO, and chromium carbide was regarded as a single-phase Cr_7C_3. According to the figure, in addition to the slag, spinel solid solution, and CO gas are predicted to exist as stable phases during corrosion testing at temperatures exceeding 1700 ℃. Based on the aforementioned reaction between Cr_7C_3 and the slag components, it is considered that spinel solid solution with the composition $(Fe, Mg)(Cr, Al)_2O_4$ is formed. During this reaction process, the oxidation of carbon in the carbide is expected to generate CO gas. The bubbles observed within the Fe-Cr residue at the slag interface following the corrosion test, as shown in **Fig. 3**, can be attributed to the generation of CO gas, as predicted by the thermodynamic analysis. Furthermore, a portion of the chromium carbide was found to dissolve into the slag as CrOx, leading to an increase in the Cr level within the slag as the temperature increased.

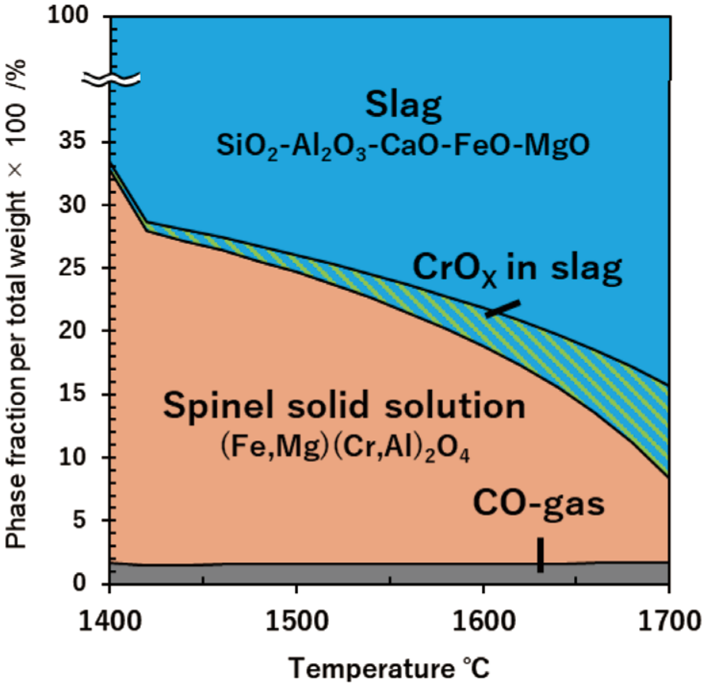

Fig. 7 Composition formed from 1400 to 1700 ℃ in the reaction of chromium carbide (Cr_7C_3) with SiO_2-CaO-Al_2O_3-FeO system slag of C/S=1, based on the thermodynamic calculation.

次にスラグとフェロクロムの反応の経過と結果を模式的に**図 8** に示す。低酸素雰囲気下での受熱で，フェロクロムはまず周囲の炭素と反応して $(Fe,Cr)_7C_3$ を生成する。次に，この炭化物がスラグと反応し，前述したように Cr の一部は CrOx として溶解し，スラグ中の Cr 濃度を上昇させる。一方で残存した炭化物は，FeO，MgO および Al_2O_3 と反応してスピネル固溶体を生成するとともに CO ガスを発生する。その結果として，スラグ接触面近傍には，Cr 炭化物残渣を核として周囲をスピネル固溶体が取り囲む特徴的な構造が形成される（**図 8** 右下図参照）。

スラグ中の Cr 濃度の上昇は，Cr 含有酸化物種の増加により粘度を上昇させる 6) 傾向があること，そして生成したスピネル固溶体はスラグ中に懸濁相として分散することにより，見掛粘度を増大させる効果を有すると考えられる。さらに，CO ガス気泡の分散も，気液混相化による見掛粘度の増大をもたらし，スラグ内の対流および物質移動が抑制される。つまり，低炭素質 MgO-C れんがのスラグ接触面には高 Cr スラグ，スピネル固溶体，および

Figure 8 schematically illustrates the reaction sequence during the reaction between slag and ferrochrome. When heated in a low-oxygen atmosphere, ferrochrome initially reacts with surrounding carbon to form $(Fe, Cr)_7C_3$. This carbide then reacts with the slag, and as previously described, part of the chromium dissolves as CrOx, enriching the Cr level in the slag. At the same time, the remaining carbide reacts with FeO, MgO, and Al_2O_3 to produce spinel solid solution and generate CO gas. As a result, distinctive microstructures are formed in the vicinity of the slag contact surface, in which residual Cr-carbide particles serve as cores surrounded by spinel solid solution, as shown in the lower right of **Fig. 8**.

An increase in the Cr content within the slag tends to increase its viscosity 6) due to the enhanced formation of Cr-containing oxides. The spinel solid solution formed under these conditions is considered to increase the apparent viscosity by dispersing throughout the slag as fine solid particles suspended in the molten phase. Furthermore, the dispersion of CO gas bubbles forms a gas–liquid mixture system within the slag, which further increasing the apparent viscosity and suppressing convection and mass transport. Consequently, a high-viscosity interfacial layer composed of Cr-enriched slag, spinel solid

COガス気泡からなる高粘度の層が形成され，耐火物のさらなる溶損を効果的に抑制する保護層となったものと考えられた。フェロクロムに加えて黒鉛を添加した系（試験れんがB-3）は，スラグと固体界面の濡れ性低下とともに，MgOとの反応によるCOガス発生の促進，粘度増大効果の強化などを通してさらなる耐食性向上に寄与することにより，焼成マグクロれんがSRBに近い耐食性を示したと考えられた。

solution, and CO gas bubbles is formed at the slag contact surface of the low-carbon MgO–C brick. This layer is believed to act as an effective protective barrier, inhibiting further dissolution of the refractories. The test bricks in which graphite was additionally used to a ferrochrome-containing brick (test brick B-3) exhibited corrosion resistance approaching that of the burnt magnesia–chrome brick SRB. This enhanced corrosion resistance is attributed to reduced wettability at the slag–solid interface, increased CO gas generation through reactions with MgO, and viscosity-increasing effects.

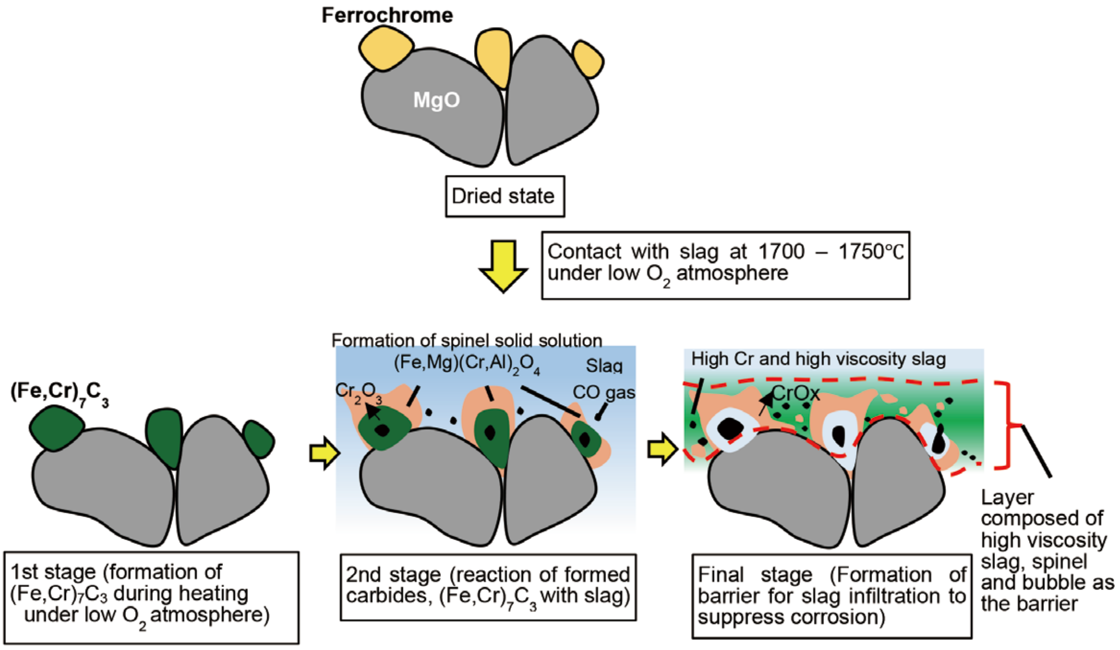

Fig. 8 Proposed mechanism to form a protection layer composed of high viscosity slag, spinel, and bubble, which is effective to reduce corrosion of refractories by suppressing slag infiltration.

4.2　実炉での適用について

フェロクロムを含むMgO-Cれんが（B（B-0））の六価クロム溶出量を環境庁告示第46号に準拠して測定した結果を**図9**に示す。250 ℃× 5h乾燥後の溶出量は規制値である0.05 mg/L未満であり，築炉作業および湿式加工時における六価クロム汚染リスクは十分に低いと考えられた。一方で，1000 ℃で熱処理した場合，CO雰囲気中では溶出量は規制値以下であるが，大気雰囲気では，溶出量は0.76 mg/Lまで増加し，焼成マグクロれんがSRBよりも少し高い値であった。一般に，六価

4･2 Application for actual furnaces

Figure 9 presents the results of Cr^{6+} elution tests conducted on MgO–C bricks containing ferrochrome (B(B-0)), in accordance with notification No.46 issued by the Ministry of the Environment. After drying at 250 ℃ for 5 h, the elution amount remained below the permissible limit of 0.05 mg/L, suggesting a sufficiently low risk of Cr^{6+} contamination during the construction and wet cutting process of bricks. When the bricks were heated at 1000 ℃ in a CO atmosphere, the amount of Cr^{6+} elution was below the permissible limit. In contrast, under an air atmosphere, it increased to 0.76 mg/L, which is slightly higher than the level of burnt magnesia–

クロム溶出はれんが中の Cr 成分が Ca と反応してクロム酸カルシウム（$CaCrO_4$）を生成することに起因し，おおむね 900 から 1000 ℃の温度域での生成増が報告されている[7]。従って前述した 1000 ℃大気中熱処理後の溶出量を想定最大溶出量とすることが妥当であると考えられる。使用後廃棄れんがにおいては，特に背面側の酸化層において焼成マグクロれんがと同等レベルの六価クロム溶出の可能性があることから，廃棄時の環境・安全面での取扱いは，焼成マグクロれんがのそれに準拠することが妥当と判断される。

chrome bricks (SRB). Cr^{6+} elution is generally attributed to the reaction between Cr components and Ca in the brick, resulting in the formation of calcium chromate ($CaCrO_4$). This reaction is known[7] to become more enhanced within the temperature range of approximately 900–1000 ℃. Therefore, the elution amount observed after heating at 1000 ℃ in air can be regarded as a reasonable estimate of the maximum potential elution amount. For used and wasted bricks, particularly in the oxidized layer on the back side of bricks, Cr^{6+} elution may occur at levels comparable to those of burnt magnesia–chrome bricks. Therefore, the disposal of such bricks should be conducted in accordance with the environmental and safety standards applied to burnt magnesia–chrome bricks.

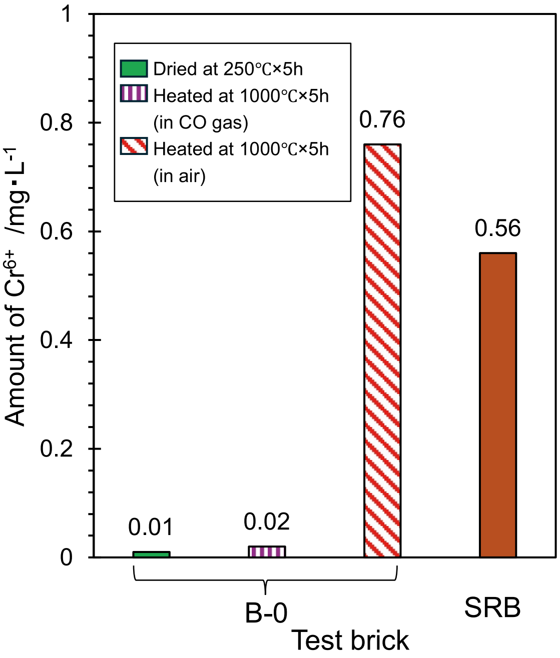

Fig. 9 Comparison of Cr^{6+} elution in the test bricks B-0 after drying at 250 ℃×5 h, heated at 1000 ℃×5 h in air and CO gas, and MgO-Cr_2O_3 brick (SRB).

表 5 にベース材 A，最も優れた耐食性を示した B-3，および焼成マグクロれんが（SRB）の耐食性と耐熱衝撃性の相対評価を示した結果を示す。低 C 質 MgO-C れんがは高 MgO 含有材であることから，低塩基度スラグに対する耐食性は焼成マグクロれんがと比較して劣る一方で，FeO に対しては優れる傾向がある。開発材 B-3 は，焼成マグクロれんがに近いスラグ耐食性を示し，ベース材 A と

Table 5 summarizes the relative evaluation results for corrosion resistance and thermal shock resistance of base brick A, the developed material B-3 with the highest corrosion resistance and burnt magnesia–chrome bricks (SRB). Due to their high MgO content, low-carbon MgO–C bricks generally exhibit inferior corrosion resistance against low-basicity slag compared to burnt magnesia–chrome bricks, while demonstrating superior resistance to FeO. The developed material B-3 showed slag

同等の耐 FeO 性を示した。しかし，クロム炭化物の生成による耐熱衝撃性の低下が認められた。

以上を踏まえ，実炉適用に際しては，低塩基度スラグかつ高酸素吹込み（OB）操業条件下において，耐火物の溶損が主要な損傷要因となる部位を対象として，焼成マグクロれんがの代替材としてB-3 を適用することが効果的であると考えられる。

corrosion resistance approaching that of burnt magnesia–chrome bricks and FeO resistance equivalent to that of base brick A. However, a decreased thermal shock resistance was observed, likely due to the formation of chromium carbides.

Based on these results, test brick B-3 is regarded as a suitable alternative for the burnt magnesia–chrome bricks in furnace areas where refractory corrosion is the main damage mechanism with low-basicity slag and high oxygen blowing (OB) operating conditions.

Table 5 Comparison of relative performance* of test brick B-3 with the comparative bricks of SRB and the base MgO-C, by assessing resistance to both corrosion and thermal shock

Test brick		SRB	A	B-3
Resistance to;		$MgO-Cr_2O_3$	MgO-C	(A)+ ferrochrome**+C***
Corrosion against	Slag****	◎	△	○
	FeO	△	○	○
Thermal shock		−	○	△

◎: excellent, ○: good, △: insufficient, **3 mass%, ***Graphite (3 mass%), ****C/S=1

5　まとめ

本研究では，二次精錬炉用 MgO-C れんがの高性能化のため，低炭素質 MgO-C れんがに各種 Cr 系材料を添加してその効果を評価した。フェロクロム粉末，Cr_2O_3 粉末，そしてクロム鉱粉末を比較した結果，フェロクロム粉末 3 mass% 添加により耐食性が 31 % 向上し，さらに黒鉛 3 mass% との併用で 64 % 改善され，現行の焼成マグクロれんがに近づいた。微構造観察と熱力学計算から，低酸素雰囲気下でフェロクロムから生成したクロム炭化物がスラグと反応してスピネル固溶体と CO ガスを生成し，スラグ接触面に高粘度保護層を形成することによる溶損抑制機構を考察した。開発材は優れた耐 FeO 性と高いスラグ耐食性を示したが，耐熱衝撃性は若干劣るため，低塩基度スラグかつ高酸素吹込み操業条件下での適用が最適であると判断された。低炭素質 MgO-C れんがにフェロクロムと黒鉛を添加することにより，従来材であるマグクロれんがと比べて製造時の CO_2 排出量低減と高耐用性がもたらされる二次精錬炉用耐火物とし

5 Conclusion

In this study, to enhance the performance of low-carbon MgO–C bricks for secondary refining furnaces, various chromium-based additives were incorporated, and their effects were evaluated. Comparative analysis of ferrochrome powder, Cr_2O_3 powder, and chrome ore powder revealed that the addition of 3 mass% ferrochrome powder improved slag corrosion resistance by 31 %. When combined with 3 mass% graphite, the improvement reached 64 %, coming close to the performance of conventional burnt magnesia–chrome bricks. Microstructural observations and thermodynamic calculations suggest that, under low-oxygen conditions, chromium carbides formed from ferrochrome react with slag to form spinel solid solutions and CO gas. This reaction contributes to the formation of a high-viscosity protective layer at the slag–refractory interface, effectively suppressing corrosion. The developed material exhibited excellent resistance to FeO and high slag corrosion resistance, although its thermal shock resistance was decreased. Therefore, its optimal application is regarded as the condition with low-basicity slag and high oxygen blowing (OB). The incorporation of ferrochrome and graphite into low-carbon MgO–C bricks demonstrate strong potential

て有望な材質となることが示された。

文献

1）Y. Tomita, T. Anan, K. Goto and K. Morikawa: Proceedings of UNITECR2023, 364-367 (2023).

2）寺田庄吾, 原　大介, 村上裕一郎, 副田知美 : 耐火物, **73** ［5］ 171-179 (2021).

3）島田岳, 平山堅太郎, 伊賀棒公一, 飯田敦久 : 環境と耐火物研究会報告集, **19** 27-35 (2020).

4）石井宏昌, 武下繁行, 佐々木王明, 前田榮造, 田中征二郎 : 耐火物, **53** ［2］ 78-79 (2001).

5）浅野敬輔, 大槻雄三, 後藤　潔, 鹿野　弘, 山本　博, 玉木健之 : 耐火物, **44** ［1］ 2-9 (1992).

6）D. Yang, F. Zhang, J. Wang, Z. Yan, G. Pei, G. Qiu, and X. Lv: Journal of Materials Research and Technology, **9** ［6］ 14673-14681 (2020).

7）山口明良 : 無機マテリアル学会 (J. of the Society of Inorganic Materials), Japan, **8** 185-190 (2001).

本報告は, 以下の報文に, 加筆, 再構成して転載したものである。

河野 颯, 清水公一, 江上雅之 : 第 13 回 鉄鋼用耐火物研究会報告集 , 耐火物技術協会 (2025) pp.96-106.

as an advanced refractory brick for secondary refining furnaces, offering both reduced CO_2 emissions during production and enhanced durability compared to conventional magnesia–chrome bricks.

References

1) Y. Tomita, T. Anan, K. Goto, and K. Morikawa: Proceedings of UNITECR2023, 364-367 (2023).

2) S. Terada, D. Hara, Y Murakami, and T. Fukuda: Taikabutsu, **73** [5] 171-179 (2021).

3) G. Shimada, K. Hirayama, K. Igabo, and A. Iida: Proceedings of Symposium on Environment and Refractories, **19** 27-35 (2020).

4) H. Ishii, S. Takeshita, K. Sasaki, E. Maeda, and S. Tanaka: Taikabutsu, **53** [2] 78-79 (2001).

5) K. Asano, Y. Otsuki, K. Goto, H. Shikano, H. Yamamoto, and K. Tamaki: Taikabutsu, **44** [1] 2-9 (1992).

6) D. Yang, F. Zhang, J. Wang, Z. Yan, G. Pei, G. Qiu, and X. Lv: Journal of Materials Research and Technology, **9** [6] 14673-14681 (2020).

7) A. Yamaguchi: Journal of the Society of Inorganic Materials, Japan, **8** 185-190 (2001).

This report is a reprint of the following report with additions and reconstruction.

Hayate Kawano, Koichi Shimizu and Masayuki Egami: Proceedings of the 13th Symposium on Refractories for Iron and Steel, Technical Association of Refractories, Japan (2025) pp.96-106.